Downregulation of microRNA-34a inhibits oxidized low-density lipoprotein-induced apoptosis and oxidative stress in human umbilical vein endothelial cells

XIAOMING ZHONG*, PENG LI*, JUAN LI, RUILI HE, GUANCHANG CHENG and YANMING LI

Department of Cardiology, Huaihe Hospital of Henan University, Kaifeng, Henan 475000, P.R. China

Received August 31, 2017; Accepted April 26, 2018

DOI: 10.3892/ijmm.2018.3663

Abstract. Oxidized low-density lipoprotein (ox-LDL) promotes endothelial cell dysfunction, which is a primary risk factor for the development of atherosclerosis. A previous study reported that microRNA (miRNA/miR)-34a is upregulated in atherosclerotic samples. However, its function and underlying mechanisms remain to be fully elucidated. In the present study, miRNA microarray analysis was performed to investigate the miRNA expression profile in atherosclerotic plaque tissues and examine the role of miR-34a in ox-LDL-induced apoptosis of human umbilical vein endothelial cells (HUVECs). Cell viability, apoptosis and protein expression was determined by a cell counting kit-8 assay, flow cytometry and western blot analysis, respectively. It was observed that miR-34a was upregulated in atherosclerotic plaque tissues and that ox-LDL treatment significantly increased the levels of miR-34a in a dose-dependent manner in the HUVECs. The knockdown of miR-34a increased the protein expression of B-cell lymphoma 2 (Bcl-2) and cell viability, improved mitochondrial membrane potential, and decreased the activity of caspase-3, number of apoptotic cells and release of cytochrome *c* from mitochondria in the ox-LDL-treated HUVECs. The results also demonstrated that the knockdown of miR-34a suppressed the levels of ox-LDL-induced reactive oxygen species (ROS) in HUVECs. Additionally, it was found that Bcl-2 was a target of miR-34a in HUVECs, and that silencing Bcl-2 abrogated the protective effects of the downregulation of miR-34a on ox-LDL-induced apoptosis. These data indicated that the knockdown of miR-34a protected against ox-LDL apoptosis and ROS in HUVECs via inhibiting the mitochondrial apoptotic pathway, suggesting it may offer potential as a biomarker in the clinical diagnosis and as a target for the treatment of atherosclerosis.

Correspondence to: Dr Yanming Li, Department of Cardiology, Huaihe Hospital of Henan University, 8 Baogonghu North Road, Kaifeng, Henan 475000, P.R. China
E-mail: liyanmingvv@sina.com

*Contributed equally

Key words: atherosclerosis, microRNA-34a, human umbilical vein endothelial cells, mitochondrial apoptotic pathway

Introduction

Atherosclerotic cardiovascular disease is the main cause of high morbidity and mortality rates worldwide (1). It has been documented that endothelial cell (EC) injury is an early step in the development of cardiovascular diseases, including myocardial infarction, cardiac failure and atherosclerosis (2). The EC injury and dysfunctions are considered to be involved in the recovery of the injured endothelium and human or animal atherosclerotic lesions via regulating EC proliferation and apoptosis, which is associated with the development of atherosclerosis (3-5). Oxidized low-density lipoprotein (ox-LDL) can cause an oxidative chain reaction and induce endothelial dysfunction, which is an essential atherosclerotic risk factor in the progression of atherosclerosis (6,7). ox-LDL has been identified to bind with the lectin-like ox-LDL receptor-1 on the endothelial cell surface, which induces apoptosis and leads to reactive oxygen species (ROS) accumulation (7). Several studies have shown that EC apoptosis is important in atherosclerosis via promoting inflammatory cell infiltration (8), neointima formation (9), lipid transport (10) and plaque rupture (11). Therefore, it is critical to protect endothelial cells against ox-LDL-induced apoptosis in the treatment of atherosclerosis.

MicroRNAs (miRNAs) are small endogenous, non-coding RNA molecules of 22-25 nucleotides, which function as unique gene expression regulators at the post-transcriptional level by repressing translation or promoting RNA degradation. Increasing evidence has shown that miRNAs are able to modulate various biological and pathological processes, including cellular differentiation, proliferation, apoptosis and carcinogenesis (12-14). A previous study demonstrated that certain miRNAs function as essential regulators in atherosclerosis by modulating crucial factors or key pathways (15). Sun *et al* (16) reported that the systemic delivery of miR-181b attenuated atherosclerosis by inhibiting NF-κB signaling in the vascular endothelium. miR-21 was shown to be associated with the progression of atherosclerosis by suppressing apoptosis and inducing proliferation in vascular smooth muscle cells (17), and another study reported that miR-513a-5p modulates tumor necrosis factor-α- and lipopolysaccharide-induced apoptosis

via downregulating X-linked inhibitor of apoptotic protein in human umbilical vein endothelial cells (HUVECs) (18). However, whether miRNAs are also involved in ox-LDL-induced EC apoptosis remains to be fully elucidated.

Several studies have shown that miR-34a has pro-apoptotic effects on various cells, including vascular ECs (19,20). A previous study revealed that miR-34a was upregulated in atherosclerotic samples (21). In the present study, miRNA microarray analysis from the Gene Expression Omnibus (GEO) database (https://www.ncbi.nlm.nih.gov/geo/query/acc.cgi?acc=GSE96621), was obtained, and it was observed that miR-34a is upregulated in atherosclerotic plaque tissues. Therefore, it was hypothesized that miR-34a may be important in the development of atherosclerosis. In the present study, the expression of miR-34a in atherosclerotic patients was further verified, and the role of miR-34a in ox-LDL-induced HUVEC apoptosis and the underlying mechanisms were investigated.

Materials and methods

Atherosclerotic serum and plaque tissue collection. A total of 25 patients with atherosclerosis and 25 healthy subjects who attended the Department of Cardiology, Huaihe Hospital of Henan University (Henan, China) were recruited between June 2015 and June 2016. Serum samples were obtained from the patients with atherosclerosis and healthy subjects for the subsequent experiments. Human advanced atherosclerotic plaques were collected during carotid endarterectomy of patients from the hospital. A total of six plaque tissues from different patients were analyzed in the present study. In addition, ascending aortas without visible atherosclerotic changes (control vessels) were sampled as controls from six patients undergoing aortic valve replacement surgery at Huaihe Hospital of Henan University. All individuals provided informed consent for the use of human specimens for clinical research. The present study was approved by the Ethics Committees of Huaihe Hospital of Henan University.

Cell culture and treatment. HUVECs (HUVEC-CS; CRL-2873; American Type Culture Collection, Manassas, VA, USA) were maintained in DMEM (Gibco; Thermo Fisher Scientific, Inc., Waltham, MA, USA) supplemented with 10% fetal bovine serum (Gibco; Thermo Fisher Scientific, Inc.), 100 U/ml penicillin and 100 μg/ml streptomycin (Sigma; EMD Millipore, Billerica, MA, USA). The cells were cultured at 37˚C in a humidified chamber containing 5% CO_2. The HUVECs were treated with different concentrations (10-200 μg/ml) of ox-LDL (Union-Bio Technology, Beijing, China) and were collected at 24 h for further measurements.

Cell transfection. The miR-34a mimics/inhibitor and mimics/inhibitor negative control (NC) were designed and synthesized by GenePharma Co., Ltd. (Shanghai, China). B-cell lymphoma 2 small interfering (si)RNA (siBcl-2; 5'-GGTACGATAACCGGGAGATAGTGAT-3) and siRNA NC (si-Scramble; 5'-GGTTAGCAAGGCGAGATATGACGAT-3') were synthesized by BioMics Biotechnologies, Co., Ltd. (Nantong, China). The HUVECs were seeded into six-well plates and transfected with miR-34a mimics/inhibitor, mimics/inhibitor NC or si-Bcl-2 using Lipofectamine 2000 (Invitrogen; Thermo Fisher Scientific, Inc.) according to the manufacturer's protocol. Following transfection for 48 h, the cells were exposed to ox-LDL (80 μg/ml) for 24 h and collected for further measurements.

RNA extraction and reverse transcription-quantitative polymerase chain reaction (RT-qPCR) analysis. Total RNA was isolated from atherosclerotic plaque tissues and cells using TRIzol reagent (Invitrogen; Thermo Fisher Scientific, Inc.) according to the manufacturer's protocol. Subsequently, the miRNA and mRNA were reverse transcribed into cDNA at 37˚C for 1 h using the Reverse Transcriptase M-MLV kit (Takara Biotechnology Co., Ltd., Dalian, China). RT-qPCR analysis was performed on an Applied Biosystems 7500 Real-Time PCR machine with miRNA-specific primers using a TaqMan Gene Expression Assay (Applied Biosystems; Thermo Fisher Scientific, Inc.). The RT-qPCR reaction system (30 μl) contained 5 μl cDNA, 10 μl mix, 1 μl upstream primer, 1 μl downstream primer and 13 μl double distilled H_2O. The PCR reaction consisted of an initial denaturation at 95˚C for 3 min, followed by 22 cycles of 95˚C for 15 sec and 60˚C for 30 sec. The U6 gene served as an endogenous control for miR-34a and β-actin served as a reference control for Bcl-2. The primers sequences were as follows: miR-34a forward, 5'-GAGACAGCCAGGAGAAATCA-3' and reverse, 5'-CCTGTGGATGACTGAGTACC-3'; Bcl-2 forward, 5'-GGATTGTGGCCTTCTTTGAG-3' and reverse, 5'-TACCCAGCCTCCGTTATCCT-3'; β-actin forward, 5'-GAGCGCGGCTACAGCTT-3' and reverse, 5'-TCCTTAATGTCACGCACGATTT-3'; U6 forward, 5'-CTCGCTTCGGCAGCACA-3' and reverse, 5'-AACGCTTCACGAATTTGCGT-3'. The miR-34a relative expression was analyzed using the $2^{-\Delta\Delta Cq}$ method (22). All reactions were performed in triplicate.

Cell viability analysis. The 3-(4,5-dimethylthiazol-2-yl)-2,5-diphenyltetrazolium bromide (MTT) assay was used to measure cell viability. Briefly, $1x10^4$ cells were seeded into 96-well plates overnight. Following transfection for 48 h, the cells were exposed to ox-LDL (80 μg/ml) for 24 h. Subsequently, 20 μl 5 mg/ml MTT solution (Sigma; EMD Millipore) was supplemented into each well and incubated for an additional 4 h. Subsequently, the supernatant was removed and 150 μl dimethylsulfoxide was added to each well. The absorbance was determined at 570 nm using a microplate reader (Tecan Group, Ltd., Männedorf, Switzerland).

Analysis of caspase-3 activation. A fluorimetric assay kit (BioVision, Inc., Milpitas, CA, USA) was used to measure the caspase-3 activity according to the manufacturer's protocol. This assay is based on the principle that activated caspases in apoptotic cells cleave the synthetic substrates to release free chromophore *p*-nitroanilide (pNA), which is measured at 405 nm. The pNA is generated following the specific action of caspase-3 on tertrapeptide substrate DEVD-pNA. In brief, the reaction mixture consisted of 50 μl of cell extract protein, 50 μl of 2X reaction buffer containing 10 mM dithiothreitol, and 5 μl of 4 mM DEVD-pNA (for caspase-3) substrate in a total volume of 105 μl. The reaction mixture was incubated at 37˚C for 1 h and the sample absorbance was determined at 405 nm using a microplate

reader (Model 680; Bio-Rad Laboratories, Inc., Hercules, CA, USA). The results were determined as fold changes compared with the control group.

Analysis of apoptosis. Following transfection for 48 h, the HUVECs were treated with 80 μg/ml of ox-LDL for 24 h. Apoptosis was measured using flow cytometry. Cells ($1x10^6$) were collected by centrifugation at 1,000 x g for 10 min at 4˚C, followed by washing of the cell pellet twice with HEPES-buffered saline. The cells were then fixed with 70% ice-cold methanol at 4˚C for 30 min. Following resuspension with binding buffer, the cells were added to 5 μl of AnnexinV-FITC and 1 μl of propidium iodide (PI; 50 μg/ml) (BD Biosciences, Franklin Lakes, NJ, USA) working solution in 100 μl cell suspension. The stained cells were analyzed using flow cytometry (FACSCalibur; BD Biosciences). The measurements were recorded at least three times in individual experiments.

Western blot analysis. Total protein from the treated HUVECs was isolated using RIPA buffer with protease inhibitor cocktail (Pierce; Thermo Fisher Scientific, Inc.). The cytosolic and mitochondrial protein extracts from the HUVECs were prepared using the Mitochondria/Cytosol fractionation kit (Enzo Life Sciences, Farmingdale, NY, USA) according to the manufacturer's protocol. The BCA Protein Assay kit (CWBiotech, Beijing, China) was used to measure the protein concentration. The protein samples (30-50 μg) were then resolved by 10 or 12% SDS-PAGE (Sigma-Aldrich; EMD Millipore) and transferred onto polyvinylidene difluoride membranes (BD Pharmingen, San Diego, CA, USA). Following blocking with 5% skimmed milk at room temperature for 1 h, the membranes were incubated with primary antibodies at 4˚C overnight against Bcl-2 (1:500; cat. no. SC-526; Santa Cruz Biotechnology, Inc., Santa Cruz, CA, USA), cleaved-caspase-3 (1:1,000; cat. no. SC-5298; Santa Cruz Biotechnology, Inc.), cleaved caspase-8 (1:1,000; cat. no. 9496; CST Biological Reagents Co., Ltd., Shanghai, China) cleaved caspase-9 (1:1,000; cat. no. ab185719; Abcam, Cambridge, MA, USA), Cytochrome *c* (Cyt *c*; 1:200; cat. no. SC-65396; Santa Cruz Biotechnology, Inc.), Bcl-2-associated X protein (Bax; 1:50; cat. no. SC-526; Santa Cruz Biotechnology, Inc.), cleaved-poly (ADP-ribose) polymerase (PARP; 1:1,000; cat. no. SC-56196; Santa Cruz Biotechnology, Inc.), gp91 (1:1,000; cat. no. SC-5827; Santa Cruz Biotechnology, Inc.) and p22phox (1:200; cat. no. SC-271968; Santa Cruz Biotechnology, Inc.) at 4˚C overnight. The β-actin (1:1,000; cat. no. SC-47778; Santa Cruz Biotechnology, Inc.) and Cyt *c* oxidase (Cox) IV (1:1,000; cat no. ab14744; Abcam) antibodies served as the internal controls for protein loading. Following this, membranes were incubated with goat anti-mouse IgG horseradish peroxidase secondary antibody (1:500; cat. no. SC-2005; Santa Cruz Biotechnology, Inc.) for 1 h at room temperature. Subsequently, the protein bands were scanned on X-ray film using an enhanced chemiluminescence detection system (PerkinElmer, Inc., Waltham, MA, USA). The relative intensity of each band on the western blots was determined using Alpha Imager 2200 software version 3.1.2 (Alpha Innotech Corporation, San Leandro, CA, USA). The measurements were taken five times on three separate occasions.

Measurement of mitochondrial membrane potential. The loss of mitochondrial membrane potential was determined via the fluoroprobe (JC-1) as previously described (23). The cultured cells were incubated with 2.0 μg/ml of JC-1 fluoroprobe at 37˚C for 30 min. Following washing with ice-cold PBS, the hepatocytes were visualized on a Nikon Eclipse TE2000 inverted microscope (Nikon Corporation, Tokyo, Japan; x400 magnification). The mitochondrial membrane potential drives the formation of red fluorescing JC-1 dimers. The ratio of red fluorescent dimers to green fluorescent monomers was evaluated through comparing the red fluorescence intensity (Ex/Em: 580/590 nm) to green fluorescence intensity (Ex/Em: 510/527 nm) using a Bio-Tek fluorescent microplate reader (Bio-Tek Instruments, Inc., Winooski, VT, USA).

Intracellular ROS measurement. The effects of miR-34a on intracellular ROS levels were measured using a total ROS detection kit (BioVision, Inc., Milpitas, CA, USA) according to the manufacturer's protocol. Briefly, the HUVECs were collected and washed with PBS. Subsequently, the cells were incubated with 500 μl ROS detection solution and stained at 37˚C for 30 min in the dark. The staining solution was replaced with PBS, and the samples were analyzed by flow cytometry.

Luciferase reporter assay. The potential binding site between Bcl-2 and miR-34a was searched using TargetScan (http://www.targetscan.org). The miR-34a mimics/inhibitor and corresponding NC were synthesized by GenePharma Co., Ltd. The fragment of the 3'-untranslated region (UTR) of Bcl-2 containing the putative wild-type (wt) binding sites and mutated (mut) binding sites for miR-34a was amplified and cloned into the pMIR-REPORT luciferase vector (Ambion; Thermo Fisher Scientific, Inc.). Site-directed mutagenesis of the Bcl-2 3'-UTR at the putative miR-34a binding site was performed using a QuikChange kit (Qiagen, Inc., Valencia, CA, USA). Subsequently, the HUVECs ($2x10^5$/well) were seeded into 24-well plates and co-transfected with 0.8 μg of pMIR-Bcl-2-3'-UTR or pMIR-Bcl-2-mut-3'-UTR, 50 nM miR-34a mimic/inhibitor or corresponding NC using Lipofectamine 2000 reagent (Invitrogen; Thermo Fisher Scientific, Inc.). At 48 h post-transfection, the luciferase activity was measured using a Dual-Light luminescent reporter gene assay (Applied Biosystems; Thermo Fisher Scientific, Inc.). The ratio of *Renilla* luciferase to Firefly luciferase was calculated for each well. Each experiment was performed at least three times in individual experiments.

Statistical analysis. All statistical analyses were performed using SPSS 14.0 software (SPSS, Inc., Chicago, IL, USA). Each experiment was performed five times on three separate occasions. Numerical data are presented as the mean ± standard error of the mean. The results were evaluated using Student's t test. $P<0.05$ was considered to indicate a statistically significant difference.

Results

miR-34a is upregulated in human atherosclerotic plaques and serums. To examine the potential involvement of miRNAs in atherosclerosis, the miRNA expression profiles were

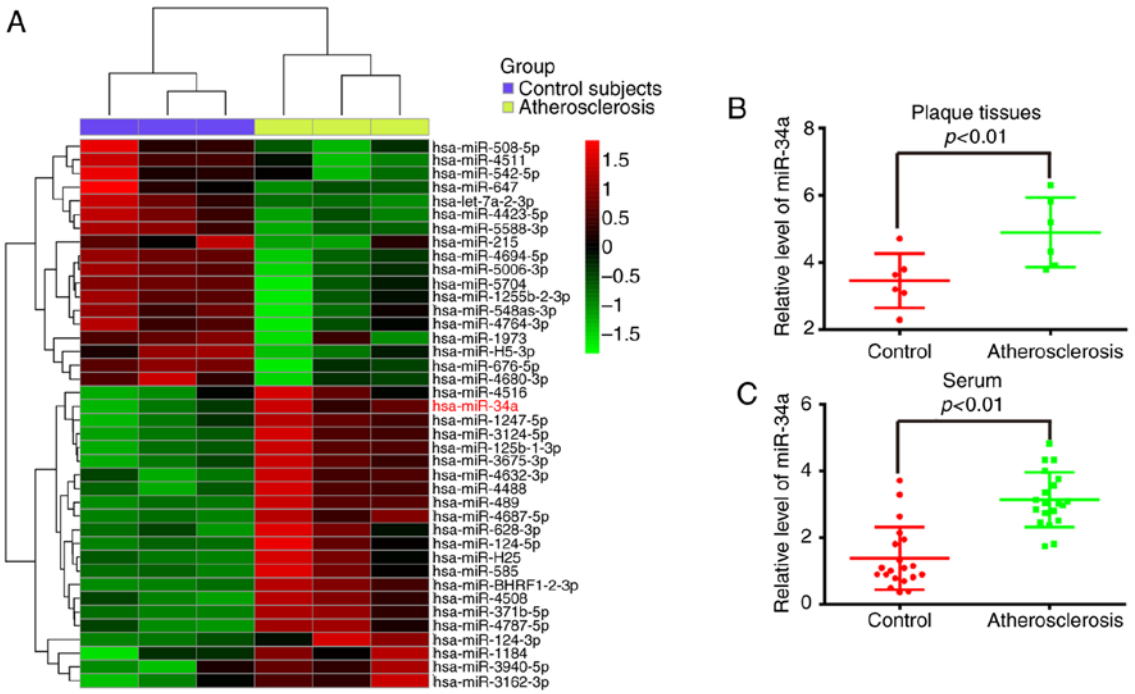

Figure 1. miR-34a is upregulated in atherosclerotic plasma samples. (A) Microarray data obtained from the Gene Expression Omnibus database (https://www.ncbi.nlm.nih.gov/geo/query/acc.cgi?acc=GSE96621). The heat map shows miRNA expression profiles in serum from patients with atherosclerosis (n=3) and without atherosclerosis (n=3). The color code is linear within the heat map: Green represents the lowest level of expression and red the highest. The upregulated miRNAs are shown from green to red, whereas the downregulated miRNAs are shown from red to green. (B) Expression of miR-34a was measured using RT-qPCR analysis in the plaque tissues from patients with atherosclerosis (n=6) and healthy subjects (n=6). (C) Levels of miR-34a were measured using RT-qPCR analysis in the serum samples form patients with atherosclerosis (n=25) and healthy subjects (n=25). Data are presented as the mean ± standard deviation of three individual experiments (**P<0.001, vs. control). miR, microRNA; RT-qPCR, reverse transcription-quantitative polymerase chain reaction.

obtained from the GEO database (https://www.ncbi.nlm.nih.gov/geo/query/acc.cgi?acc=GSE96621), which exhibited the microarray profiles of atherosclerotic and non-atherosclerotic serum of patients. Several miRNAs were altered in the patients with atherosclerosis and miR-34a was one of the miRNAs identified as being upregulated most markedly, compared with the patients without atherosclerosis (Fig. 1A). A previous study also identified miR-34a as being overexpressed in atherosclerotic samples (21). To further validate these results, atherosclerotic plaques and control vessels were collected, and miR-34a was identified using RT-qPCR analysis. It was found that the level of miR-34a was significantly upregulated in the atherosclerotic plaques, compared with that in the control vessels (P<0.01; Fig. 1B). The results further verified that miR-34a was upregulated in the serum of patients with atherosclerosis, compared with that of the control (P<0.01; Fig. 1C). These data indicated that miR-34a may be important in atherosclerotic progression and function as a biomarker in the clinical diagnosis of atherosclerosis.

Knockdown of miR-34a prevents ox-LDL-induced HUVEC apoptosis. As a model for investigations involving ECs, HUVECs (HUVEC-CS) are widely used in the investigation of atherosclerosis (18,24,25). To investigate the effect of miR-34a on the development of atherosclerosis, the HUVEC model was established, which was treated with different concentrations (10-200 μg/ml) of ox-LDL for 24 h, and the level of miR-34a was measured using RT-qPCR analysis. It was found that treatment with 10-200 μg/ml of ox-LDL increased the levels of miR-34a in a dose-dependent manner in the HUVECs (Fig. 2A). miR-34a was increased 273.92±23.07% at 80 μg/ml ox-LDL for 24 h, compared with blank group. Therefore, this concentration was selected in subsequent experiments. Firstly, the inhibition efficiency of miR-34a inhibitor and overexpression efficiency of miR-34a mimic were investigated in HUVECs transfected with miR-34a mimic/inhibitor or mimic/inhibitor NC. As shown in Fig. 2B, transfection with miR-34a mimic/inhibitor resulted in the upregulation and downregulation of miR-34a, respectively, compared with the NC cells (P<0.01). To determine whether miR-34a can influence the effects of ox-LDL-mediated apoptosis on HUVECs, the HUVECs were treated with ox-LDL (80 μg/ml) for 24 h following transfection with miR-34a inhibitor or inhibitor NC, and an MTT assay was used to measure cell viability. The results showed that ox-LDL treatment markedly reduced the cell viability, compared with that in the blank control group, however, the ox-LDL-induced reduction in cell viability was reversed by the downregulation of miR-34a (P<0.01; Fig. 2C). As shown in Fig. 2D and E, the knockdown of miR-34a also significantly decreased the activity of caspase-3 and proportion of apoptotic cells in the ox-LDL-treated HUVECs, compared with the inhibitor NC cells (P<0.01). Additionally, to evaluate the molecular mechanisms of miR-34a-mediated apoptosis, western blot analysis was used to measure the expression levels of apoptosis-related proteins in the ox-LDL-treated HUVECs following transfection with miR-34a inhibitor or inhibitor NC. The data revealed that ox-LDL treatment markedly increased the pro-apoptotic proteins (cleaved-caspase-3, -8,

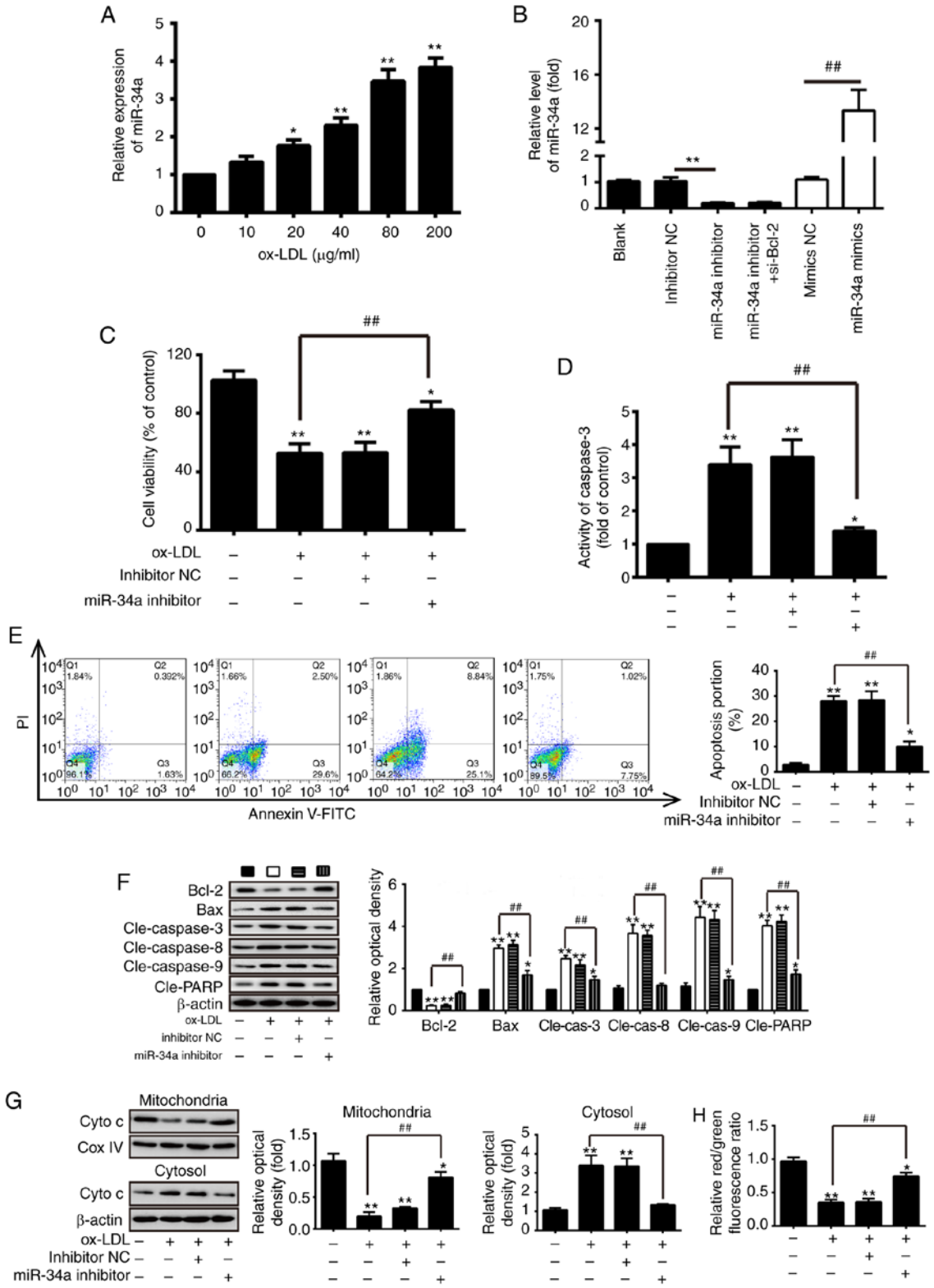

Figure 2. Knockdown of miR-34a inhibits ox-LDL-induced HUVEC apoptosis. (A) RT-qPCR analysis was performed to identify the expression of miR-34a in HUVECs following treatment with different concentrations (10-200 μg/ml) of ox-LDL for 24 h. (B) HUVECs were transfected with miR-34a mimic/inhibitor or mimic/inhibitor NC. The expression of miR-34a was measured using RT-qPCR analysis (**P<0.01, vs. inhibitor NC; $^{\#\#}$P<0.01, vs. mimic NC). (C) HUVECs were treated with 80 μg/ml of ox-LDL for 24 h following transfection with miR-34a inhibitor or inhibitor NC, and an MTT assay was performed to measure cell viability. Treated HUVECs were analyzed using a (D) fluorimetric assay kit, (E) flow cytometry and (F) western blot analyses to measure caspase-3 activity, apoptotic cells and apoptosis-related proteins (Bcl-2, cleaved-caspase-3, -8, -9, Bax and cleaved-PARP), respectively. (*P<0.05 and **P<0.01, vs. blank group; $^{\#\#}$P<0.01, vs. ox-LDL-treated group). (G) Protein levels of Cyto *c* in mitochondria and cytosol was measured using western blot analysis. β-actin and Cox IV were used as loading controls for the cytosolic and mitochondrial fractions, respectively. (*P<0.05 and **P<0.01, vs. blank group; $^{\#\#}$P<0.01, vs. ox-LDL-treated group). (H) Mitochondrial membrane potential levels in the treated HUVECs were analyzed using the JC-1 fluorescent probe. The relative red/green fluorescence ratio was obtained by Microplate Multimode Reader Modulus. Data are presented as the mean ± standard deviation of three independent experiments (*P<0.05 and **P<0.01, vs. blank group; $^{\#\#}$P<0.01, vs. ox-LDL-treated group). miR, microRNA; HUVECs, human umbilical vein endothelial cells; ox-LDL, oxidized low density lipoprotein; Bcl-2, B-cell lymphoma 2; Bax, Bcl-2-associated X protein; PARP, poly (ADP-ribose) polymerase; Cyt *c*, cytochrome *c*; COX IV, Cyto *c* oxidase IV; NC, negative control; si-, small interfering RNA; PI, propidium iodide; cle-, cleaved.

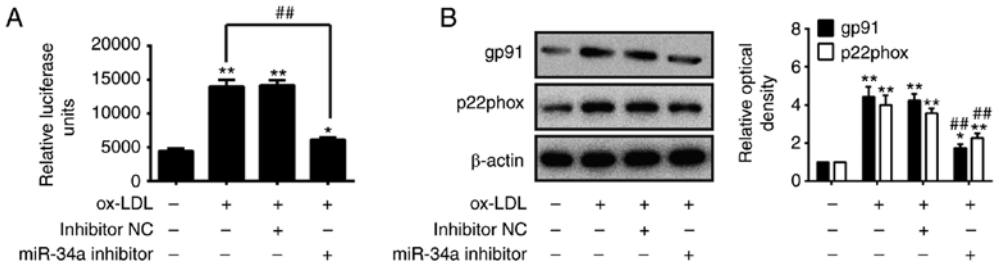

Figure 3. Knockdown of miR-34a reduces ox-LDL-induced ROS in HUVECs. (A) At 24 h post-transfection with miR-34a inhibitor or inhibitor NC, the HUVECs were treated with 80 μg/ml of ox-LDL and a ROS detection kit was used to measure ROS levels. (B) Protein levels of gp91 and p22phox were detected using western blot analysis. β-actin was used as an internal control. Data are presented as the mean ± standard deviation of three individual experiments (*P<0.05 and **P<0.01, vs. blank group; $^{\#\#}$P<0.01, vs. ox-LDL-treated group). miR, microRNA; HUVECs, human umbilical vein endothelial cells; ox-LDL, oxidized low density lipoprotein; ROS, reactive oxygen species; NC, negative control.

-9, Bax and cleaved-PARP) and decreased the protein expression of anti-apoptotic Bcl-2, compared with the blank control group (P<0.01; Fig. 2F). However, the knockdown of miR-34a significantly inhibited the expression of pro-apoptotic proteins (cleaved-caspase-3, -8, -9, Bax and cleaved-PARP) and increased the protein expression of anti-apoptotic Bcl-2, compared with the inhibitor NC group (P<0.01; Fig. 2F).

The release of Cyto *c* from mitochondria into the cytosol is a critical event in apoptosis. To further investigate the effect of miR-34a on Cyto *c* release, the HUVECs were treated with ox-LDL (80 μg/ml) for 24 h following transfection with miR-34a inhibitor or inhibitor NC, and the protein levels of Cyto *c* in the mitochondria and the cytosol was measured using western blot analysis. The results showed that ox-LDL treatment induced the release of Cyto *c* from the mitochondria, and the knockdown of miR-34a attenuated the ox-LDL-induced Cyto *c* release (P<0.01; Fig. 2G). Subsequently, mitochondrial membrane potential was analyzed using the JC-1 fluorescent probe; it was found that ox-LDL treatment significantly reduced the red/green fluorescence ratio, compared with that in the blank control cell (P<0.01; Fig. 2H). However, the knockdown of miR-34a significantly increased the red/green fluorescence ratio in the ox-LDL-treated HUVECs (P<0.01; Fig. 2H). Collectively, these data suggested that the knockdown of miR-34a protected HUVECs against ox-LDL-induced apoptosis via inhibiting the mitochondrial apoptotic pathway.

Knockdown of miR-34a protects against ox-LDL-induced ROS. A previous study revealed that ROS is associated with the initiation and progression stages of atherogenesis (25). Therefore, the present study investigated the effects of miR-34a on ROS induced by ox-LDL in HUVECs. The HUVECs were treated with 80 μg/ml of ox-LDL for 24 h following transfection with miR-34a inhibitor or inhibitor NC, and the ROS levels were determined using a ROS detection kit. As shown in Fig. 3A, ox-LDL treatment markedly increased the ROS levels, compared with those in the blank control group, however, the ROS levels were significantly decreased by the knockdown of miR-34a, compared with the ox-LDL-treated group (P<0.01; Fig. 3A). To confirm the anti-oxidative effects of the downregulation of miR-34a, western blot analysis was performed to detect the expression level of oxidative injury-related proteins gp91 (NOX2) and p22phox (26). As shown in Fig. 3B, the knockdown of miR-34a markedly reduced the expression of gp91 and p22phox in the ox-LDL-treated HUVECs (P<0.01; Fig. 3B). These results suggested that the knockdown of miR-34a exerted anti-oxidative effects against ox-LDL-induced ROS levels in the HUVECs.

miR-34a inhibits the expression of Bcl-2 by targeting its 3'-UTR in HUVECs. Previous studies have found that miR-34a exerts pro-apoptotic effects by targeting anti-apoptotic protein Bcl-2 in various types of cancer (27,28). Therefore, it was hypothesized that ox-LDL-induced HUVEC apoptosis was regulated by miR-34a via suppressing Bcl-2. The target gene of miR-34a was predicted using bioinformatics analysis. It was found that miR-34a may regulate Bcl-2 by binding with its 3'-UTR (Fig. 4A). As shown in Fig. 4B, compared with the mimic NC group, miR-34a mimics markedly repressed the luciferase activity in the presence of the wt 3'-UTR, however, the miR-34a inhibitor markedly increased the luciferase activity (P<0.01; Fig. 4B), whereas no inhibition of luciferase activity was found for the mut 3'UTR group (Fig. 4B). To verify that Bcl-2 was negatively modulated by miR-34a, western blot and RT-qPCR analyses were performed to detect the protein and mRNA levels of Bcl-2 in HUVECs transfected with miR-34a mimic/inhibitor or corresponding NC, respectively. The results demonstrated that the overexpression of miR-34a markedly reduced Bcl-2 at the protein and mRNA levels, whereas the knockdown of miR-34a led to a significant increase in the protein and mRNA levels of Bcl-2, compared with those in the NC group (P<0.01; Fig. 4C and D). RT-qPCR analysis was used to detect the mRNA levels of Bcl-2 in atherosclerotic plaque tissues (n=6), and it was found that the expression of Bcl-2 was significantly decreased in the plaque tissues, compared with that in the control (P<0.01; Fig. 4E). The results also verified that the mRNA level of Bcl-2 was downregulated in the serum of patients with atherosclerosis (n=25; P<0.01; Fig. 4F). The correlation analysis showed a negative association between the expression of Bcl-2 and the expression of miR-34a in serum samples from the patients with atherosclerosis (r=-0.8404, P<0.001; Fig. 4G). Taken together, these data indicated that miR-34a repressed Bcl-2 via targeting its 3'-UTR in HUVECs, suggesting that miR-34a may induce HUVEC apoptosis in atherosclerosis through targeting Bcl-2.

Silencing Bcl-2 inhibits the protective effects of the downregulation of miR-34a on ox-LDL-induced HUVEC apoptosis. The present study evaluated the interference efficiency of

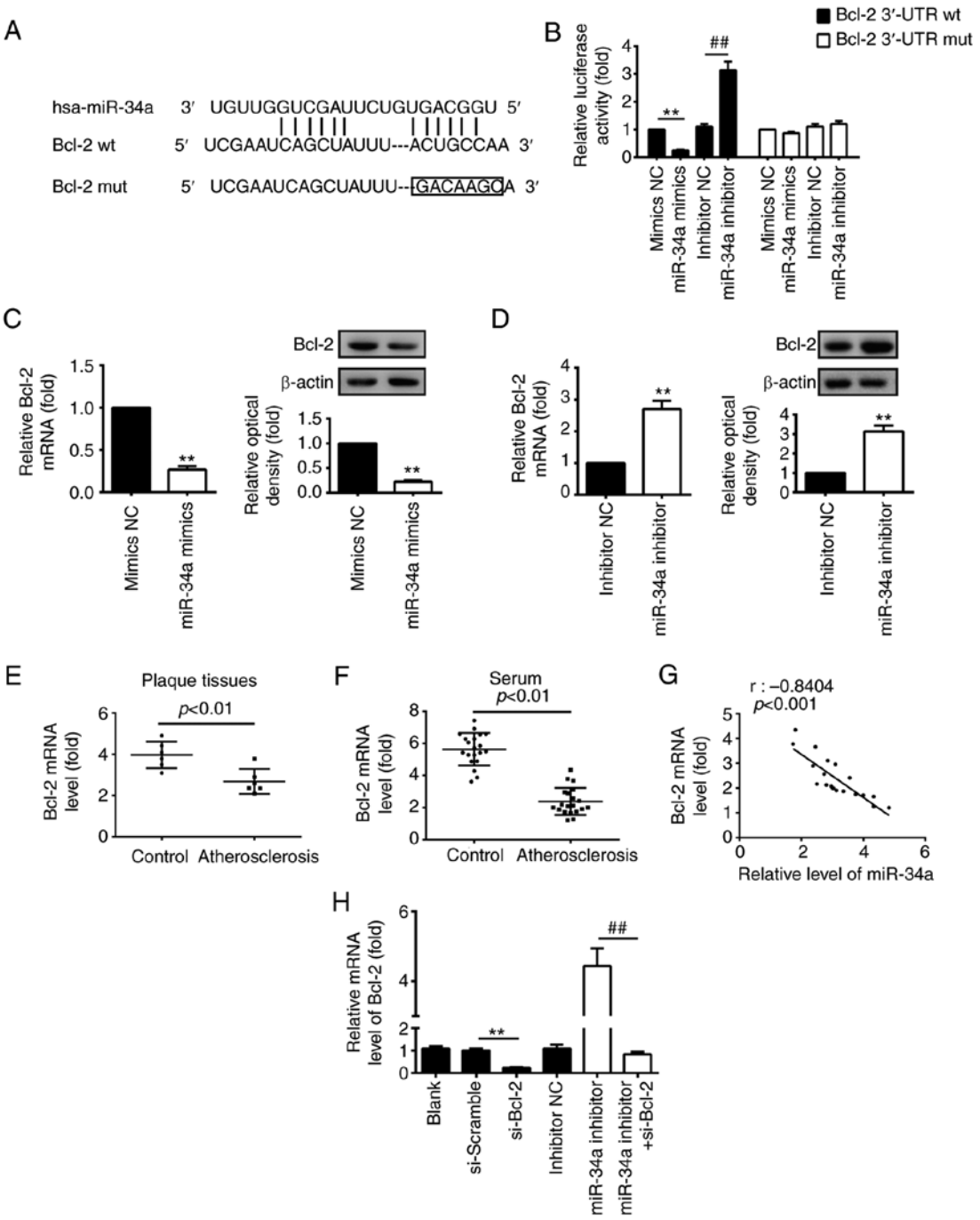

Figure 4. Bcl-2 is a direct target of miR-34a in HUVECs. (A) Putative miR-34a binding sites on 3'-UTR of Bcl-2 mRNA were predicted using TargetScan. (B) Relative luciferase activity of Bcl-2 wt or mut 3'-UTR in HUVECs following transfection with the miR-34a mimic, inhibitor or corresponding NC (**P<0.01, vs. mimic NC; $^{\#\#}$P<0.01, vs. inhibitor NC). HUVECs were transfected with (C) miR-34a mimic or (D) inhibitor, or corresponding NC, the protein and mRNA levels of Bcl-2 were measured using a western blot assay and RT-qPCR analysis, respectively (**P<0.01, vs. corresponding NC). β-actin was used as an internal control. (E) RT-qPCR analysis was used to determine the mRNA expression of Bcl-2 in atherosclerotic plaque tissues (n=6). (F) RT-qPCR analysis was used to determine the mRNA expression of Bcl-2 in serum samples from patients with atherosclerosis (n=20) and control subjects (n=20). (G) Negative correlation between levels of Bcl-2 and miR-34a in serum samples from patients with atherosclerosis and control subjects (n=20; r=-0.8404, P<0.001). Data are presented as the mean ± standard deviation of three individual experiments. (H) HUVECs were transfected with si-Bcl-2 and si-Scramble, or co-transfected with miR-34a inhibitor and si-Bcl-2. RT-qPCR analysis was used to detect the mRNA level of Bcl-2 in HUVECs (**P<0.01, vs. si-Scramble; $^{\#\#}$P<0.01, vs. miR-34a inhibitor). Data are presented as the means ± standard deviation of three individual experiments. miR, microRNA; HUVECs, human umbilical vein endothelial cells; UTR, untranslated region; Bcl-2, B-cell lymphoma 2; si-, small interfering RNA; wt, wild-type; mut, mutant; NC, negative control; RT-qPCR, reverse transcription-quantitative polymerase chain reaction.

si-Bcl-2 in HUVECs transfected with si-Bcl-2 or si-Scramble, or co-transfected with miR-34a inhibitor and si-Bcl-2. As shown in Fig. 4H, si-Bcl-2 interfered with the expression of Bcl-2, compared with that in the si-Scramble group (P<0.01). In addition, the inhibition of miR-34a significantly increased the expression of Bcl-2, whereas silencing Bcl-2 eliminated the effect of the miR-34a inhibitor-induced upregulation of Bcl-2 in HUVECs co-transfected with miR-34a inhibitor and

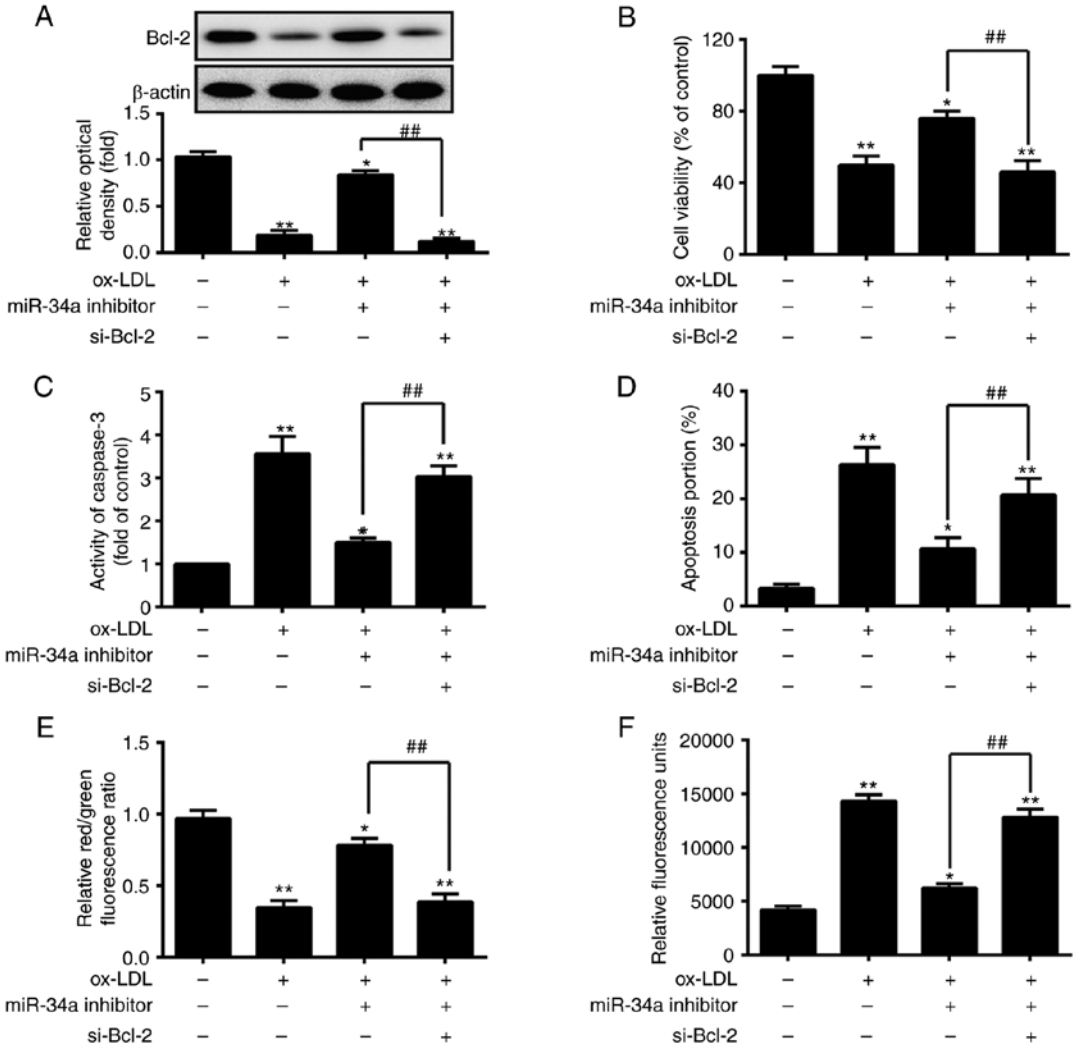

Figure 5. Silencing Bcl-2 suppresses the protective effects of the downregulation of miR-34a on ox-LDL-induced HUVEC apoptosis. The HUVECs were treated with 80 μg/ml of ox-LDL for 24 h following co-transfection with miR-34a inhibitor and si-Bcl-2 or transfection with either miR-34a inhibitor or si-Bcl-2. (A) Western blot analysis, an (B) MTT assay, (C) fluorimetric assay, (D) flow cytometric analysis, (E) JC-1 fluorescent probe and a (F) ROS detection kit were used to measure the expression of Bcl-2, cell viability, caspase-3 activity, apoptotic cells, mitochondrial membrane potential and ROS levels, respectively. Data are presented as the mean ± standard deviation of three individual experiments (*P<0.05 and **P<0.01, vs. blank group; $^{\#\#}$P<0.01, vs. ox-LDL-treated group). miR, microRNA; HUVECs, human umbilical vein endothelial cells; Bcl-2, B-cell lymphoma 2; si-, small interfering RNA; ox-LDL, oxidized low density lipoprotein; ROS, reactive oxygen species; NC, negative control.

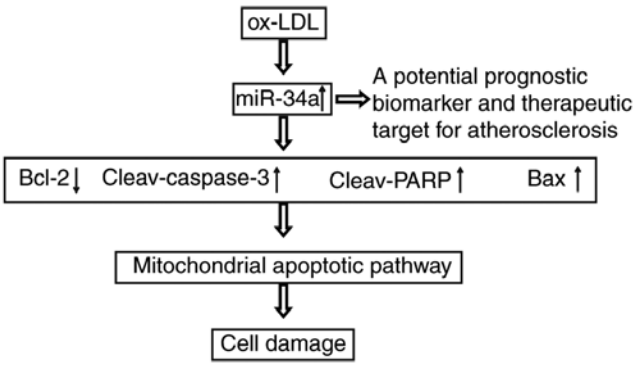

Figure 6. Mechanism schematic. Upregulation of miR-34a is induced by ox-LDL in human umbilical vein endothelial cells. miR-34a then inhibits the target gene Bcl-2, and upregulates the apoptotic proteins cleaved-caspase-3, Bax and cleaved-PARP. Finally, the overexpression of miR-34a aggravates ox-LDL-induced cell damage via activating the mitochondrial apoptotic pathway. miR, microRNA; ox-LDL, oxidized low density lipoprotein; Bcl-2, B-cell lymphoma 2; Bax, Bcl-2-associated X protein; PARP, poly (ADP-ribose) polymerase; cleav-, cleaved.

si-Bcl-2 (P<0.01; Fig. 4H). Subsequently, to verify whether the protective effects of the downregulation of miR-34a on ox-LDL-induced apoptosis is modulated by the expression of Bcl-2, the HUVECs were co-transfected with miR-34a inhibitor and si-Bcl-2 or were transfected with either the miR-34a inhibitor or si-Bcl-2 prior to ox-LDL treatment. Western blot analysis, an MTT assay, a fluorimetric assay, flow cytometric analysis, the JC-1 fluorescent probe and a ROS detection kit were then used to measure the expression of Bcl-2, cell viability, caspase-3 activity, apoptotic cells, mitochondrial membrane potential and ROS levels, respectively. Consistent with the above results, the knockdown of miR-34a increased the protein expression of Bcl-2, cell viability and the red/green fluorescence ratio, and decreased the activity of caspase-3, apoptotic cells and ROS levels in the ox-LDL-treated HUVECs. The effects of the downregulation of miR-34a on the ox-LDL-treated HUVECs were eliminated by silencing Bcl-2 (P<0.01; Fig. 5A-F). These results indicated

that the protective effects of the downregulation of miR-34a on ox-LDL-induced HUVEC apoptosis were weakened by silencing Bcl-2.

Discussion

A previous study documented that certain specific miRNAs are involved in the progression of atherosclerosis by modulating the properties of vascular cells and different cellular functions (29), and their expression have been closely associated with the pathogenesis of atherosclerosis (29). A previous study reported that the upregulation of miR-876 induced EC apoptosis in the development of atherosclerosis by repressing anti-apoptotic protein Bcl-extra large (Bcl-xL) (30). Zhang *et al* (25) demonstrated that the inhibition of miR-155 improved high glucose-induced EC injury by suppressing the activation of nuclear factor-κB. miR-34a is upregulated in atherosclerotic samples and is involved in the progression of atherosclerosis (21), in addition to possessing pro-apoptotic effects on ECs (20). Previous miRNA microarray analysis confirmed that the levels of miR-34a are increased in the serum of patients with atherosclerosis. However, the potential molecular mechanism of miR-34a in atherosclerosis requires further investigation to be fully elucidated. In the present study, the expression of miR-34a was further validated in atherosclerotic plaque tissues and the underlying mechanisms of miR-34a in ox-LDL-induced HUVEC apoptosis were examined. It was found that miR-34a was upregulated in the atherosclerotic plaque tissues. The results also demonstrated that ox-LDL treatment increased the levels of miR-34a in a dose-dependent manner, and that the knockdown of miR-34a inhibited ox-LDL-induced apoptosis and ROS levels in the HUVECs. In addition, Bcl-2 was identified as a direct target of miR-34a, and silencing Bcl-2 abrogated the protective effects of the downregulation of miR-34a on ox-LDL-induced apoptosis in HUVECs.

It has been confirmed that ox-LDL is an important factor in the initiation and progression of atherosclerosis (31). Ox-LDL has also been identified as being increased in diabetic patients, causing atherogenesis and endothelial damage (32). Additionally, ox-LDL promotes the recruitment of monocytes by vascular cells and triggers their differentiation into macrophages (33). Ox-LDL is able to induce monocyte adhesion, ROS generation and apoptosis in vascular ECs via binding the lectin-like endothelial ox-LDL receptor (LOX-1) (34-36). However, the mechanism underlying ox-LDL-mediated HUVEC apoptosis remain to be fully elucidated.

Chen *et al* (37) reported that miR-98 inhibits proliferation and decreases ox-LDL-induced apoptosis through targeting LOX-1 in HUVECs. miR-26a protects ECs from ox-LDL-induced apoptosis in the setting of atherosclerosis by targeting transient receptor potential cation channel subfamily C member 6 (38). The natural product 2,4,5-trihydroxybenzaldehyde has been found to effectively inhibit oxygen-glucose deprivation/reperfusion-induced EC injury via suppressing miR-34a (20). Therefore, it was hypothesized that miR-34a may modulate ox-LDL-mediated apoptosis in HUVECs. RT-qPCR analysis was used to measure the expression of miR-34a in HUVECs treated with different concentration (10-200 μg/ml) of ox-LDL. The results indicated that ox-LDL treatment increased the levels of miR-34a in a dose-dependent manner, suggesting that miR-34a is important in ox-LDL-induced apoptosis. It was also observed that ox-LDL treatment reduced cell viability, and increased the activity of caspase-3 and the number of apoptotic cells, whereas the downregulation of miR-34a increased cell viability, and reduced the activity of caspase-3 and apoptotic cells in the ox-LDL-treated HUVECs. These data indicated that the downregulation of miR-34a protected against ox-LDL-induced apoptosis in HUVECs.

Oxidative stress is a potent pathogenic mechanism in atherosclerosis via inducing apoptosis, mitochondria dysfunction and cellular injury (39,40). Oxidative stress is considered as the increased bioactivity of ROS relative to antioxidant defenses (41). ROS have been identified to act as a major trigger of EC apoptosis (42). Zhang *et al* (43) revealed that miR-34a/sirtuin-1/foxo3a exerts an important function in genistein in preventing ox-LDL-induced oxidative damage in HUVECs. According to these findings, the present study examined whether the knockdown of miR-34a ameliorates ox-LDL-induced apoptosis via modulating ROS, and examined the protective effects of the downregulation of miR-34a on oxidative injury. The results demonstrated that the knockdown of miR-34a reduced ox-LDL-induced ROS levels in the HUVECs. Various enzymatic sources within the myocardium are capable of producing excess ROS, including nicotinamide adenine dinucleotide phosphate (NADPH). NADPH oxidases are multimeric enzymes, which contain a membrane-bound core, comprising a catalytic gp91phox subunit (NOX2) and a p22phox subunit (44). Li *et al* (45) revealed that miR-34a induced apoptosis and enhanced the production of ROS in a human glioma cell via targeting NOX2. In the present study, the results demonstrated that the downregulation of miR-34a attenuated the expression of gp91 and p22phox in the ox-LDL-treated HUVECs. However, further investigation is required to determine the factors underlying the possible pathway of miR-34a-regulated expression of gp91 and p22phox in HUVECs. These findings suggested that the knockdown of miR-34a exerted protective effects against ox-LDL-induced HUVEC injury via suppressing the production of ROS.

Apoptosis, or programmed cell death, is important in physiological and pathological conditions, and ox-LDL-induced EC apoptosis is considered to be key in atherosclerosis (46). EC apoptosis is also involved in atherosclerotic plaque development and progression (47). The balance of Bcl-2 family members, including anti-apoptotic proteins Bcl-xL and Bcl-2, and pro-apoptotic proteins Bcl-2-associated death promoter, Bcl-2 homologous antagonist/killer, and Bax, is disrupted, which is a vital mechanism that contributes to apoptosis (48). A previous study demonstrated that miR-1907 aggravates atherosclerosis-associated EC apoptosis by inhibiting Bcl-2 (49). It has been extensively reported that Bcl-2 is a direct target of miR-34a in various cells (27,28,50,51). In the present study, the results confirmed that miR-34a suppressed the expression of Bcl-2 by directly targeting its 3'-UTR in HUVECs. Furthermore, silencing Bcl-2 impaired the protective effects of the downregulation of miR-34a on ox-LDL-induced apoptosis. Collectively, these data suggested that miR-34a regulated ox-LDL-induced apoptosis by targeting the anti-apoptotic protein Bcl-2 in HUVECs.

Mitochondria-mediated apoptosis, an intrinsic pathway of apoptosis, is usually activated by loss of mitochondrial membrane potential, and proceeds through the release of Cyto *c* and ROS from the intermembraneous space of the mitochondria to the cytosol (52). Mitochondrial dysfunction can result in the release of Cyto *c* into the cytosol, where it forms a complex with apoptotic peptidase activating factor 1, which subsequently recruits and activates procaspase-9 into active caspase-9 (53,54). Caspase-9 cleaves and activates procaspase-3, a downstream executioner caspase protein, which cleaves various 'death substrates' and thereby triggers the apoptotic cell phenotype. A previous study demonstrated that the knockdown of miR-34a altered the integrity of the mitochondrial outer membrane and increased the release of Cyto *c* from mitochondria, finally activating the caspase-mediated apoptotic pathway in vascular ECs (20). In the present study, the results showed that the knockdown of miR-34a inhibited cleaved-caspase-3, -8, -9, Bax and cleaved-PARP, and increased Bcl-2 in the ox-LDL-treated HUVECs. In addition, the knockdown of miR-34a attenuated the ox-LDL-induced release of Cyto *c* and improved mitochondrial membrane potential. Taken together, these findings indicated that the ox-LDL-mediated upregulation of miR-34a induced HUVEC apoptosis via activating the apoptotic pathway (Fig. 6), suggesting it offers potential as a prognostic biomarker and therapeutic target for atherosclerosis.

In conclusion, the results of the present study demonstrated that miR-34a was upregulated in atherosclerotic plaque tissues, and that the knockdown of miR-34a prevented ox-LDL-induced HUVEC apoptosis by increasing cell viability, decreasing caspase-3 activity, and inhibiting apoptotic cells and ROS. In addition, miR-34a modulated ox-LDL-induced apoptosis by repressing anti-apoptotic protein Bcl-2 in the HUVECs. These findings indicated that the knockdown of miR-34a protected against ox-LDL-induced apoptosis and oxidative stress via inhibiting the mitochondrial apoptotic pathway, suggesting that miR-34a serves as a biomarker in the clinical diagnosis and treatment of atherosclerosis.

Acknowledgements

Not applicable.

Funding

No funding was received.

Availability of data and materials

All data generated or analyzed during this study are included in this published article.

Authors' contributions

XZ and PL and performed the experiments, contributed to data analysis and wrote the paper. JL, RH and GC analyzed the data. YL conceptualized the study design, contributed to data analysis and experimental materials. All authors read and approved the final manuscript.

Ethics approval and consent to participate

All individuals provided informed consent for the use of human specimens for clinical research. The present study was approved by Huaihe Hospital of Henan University Ethics Committees.

Consent for publication

Not applicable.

Competing interests

The authors declare that they have no competing interests.

References

1. Go AS, Mozaffarian D, Roger VL, Benjamin EJ, Berry JD, Blaha MJ, Dai S, Ford ES, Fox CS, Franco S, *et al*: Executive summary: Heart disease and stroke statistics-2014 update: A report from the American Heart Association. Circulation 129: 399-410, 2014.
2. Tabas I, Williams KJ and Borén J: Subendothelial lipoprotein retention as the initiating process in atherosclerosis. Circulation 116: 1832-1834, 2007.
3. Otsuka F, Finn AV, Yazdani SK, Nakano M, Kolodgie FD and Virmani R: The importance of the endothelium in atherothrombosis and coronary stenting. Nat Rev Cardiol 9: 439-453, 2012.
4. Pober JS and Sessa WC: Evolving functions of endothelial cells in inflammation. Nat Rev Immunol 7: 803-815, 2007.
5. Stoneman VE and Bennett MR: Role of apoptosis in atherosclerosis and its therapeutic implications. Clin Sci 107: 343, 2004.
6. Sawamura T, Kume N, Aoyama T, Moriwaki H, Hoshikawa H, Aiba Y, Tanaka T, Miwa S, Katsura Y, Kita T, *et al*: An endothelial receptor for oxidized low-density lipoprotein. Nature 386: 73-77, 1997.
7. Cominacini L, Rigoni A, Pasini AF, Garbin U, Davoli A, Campagnola M, Pastorino AM, Lo Cascio V and Sawamura T: The binding of oxidized low density lipoprotein (ox-LDL) to ox-LDL receptor-1 reduces the intracellular concentration of nitric oxide in endothelial cells through an increased production of superoxide. J Biol Chem 276: 13750-13755, 2001.
8. Choy JC, Granville DJ, Hunt DW and McManus BM: Endothelial cell apoptosis: Biochemical characteristics and potential implications for atherosclerosis. J Mol Cell Cardiol 33: 1673-1690, 2001.
9. Zhang L, Sivashanmugam P, Wu JH, Brian L, Exum ST, Freedman NJ and Peppel K: Tumor necrosis factor receptor-2 signaling attenuates vein graft neointima formation by promoting endothelial recovery. Arterioscler Thromb Vasc Biol 28: 284-289, 2008.
10. von Eckardstein A and Rohrer L: Transendothelial lipoprotein transport and regulation of endothelial permeability and integrity by lipoproteins. Curr Opin Lipidol 20: 197-205, 2009.
11. Kavurma MM, Bhindi R, Lowe HC, Chesterman C and Khachigian LM: Vessel wall apoptosis and atherosclerotic plaque instability. J Thromb Haemost 3: 465-472, 2005.
12. Bartel DP: MicroRNAs: Genomics, biogenesis, mechanism, and function. Cell 116: 281-297, 2004.
13. le Sage C and Agami R: Immense promises for tiny molecules: Uncovering miRNA functions. Cell Cycle 5: 1415-1421, 2006.
14. Croce CM: Causes and consequences of microRNA dysregulation in cancer. Nature Rev Genet 10: 704-714, 2009.
15. Menghini R, Stöhr R and Federici M: MicroRNAs in vascular aging and atherosclerosis. Ageing Res Rev 17: 68-78, 2014.
16. Sun X, He S, Wara AKM, Icli B, Shvartz E, Tesmenitsky Y, Belkin N, Li D, Blackwell TS, Sukhova GK, Croce K and Feinberg MW: Systemic delivery of microrna-181b inhibits nuclear factor-kB activation, vascular inflammation, and atherosclerosis in apolipoprotein E-deficient mice. Circ Res 114: 32-40, 2014.
17. Lin Y, Liu X, Cheng Y, Yang J, Huo Y and Zhang C: Involvement of microRNAs in hydrogen peroxide-mediated gene regulation and cellular injury response in vascular smooth muscle cells. J Biol Chem 284: 7903-7913, 2009.

18. Shin S, Moon KC, Park KU and Ha E: MicroRNA-513a-5p mediates TNF-α and LPS induced apoptosis via downregulation of X-linked inhibitor of apoptotic protein in endothelial cells. Biochimie 94: 1431-1436, 2012.
19. Li QL, Zhang HY, Qin YJ, Meng QL, Yao XL and Guo HK: MicroRNA-34a promoting apoptosis of human lens epithelial cells through down-regulation of B-cell lymphoma-2 and silent information regulator. Int J Ophthalmol 9: 1555-1560, 2016.
20. Liao LX, Zhao MB, Dong X, Jiang Y, Zeng KW and Tu PF: TDB protects vascular endothelial cells against oxygen-glucose deprivation/reperfusion-induced injury by targeting miR-34a to increase Bcl-2 expression. Sci Rep 6: 37959, 2016.
21. Raitoharju E, Lyytikäinen LP, Levula M, Oksala N, Mennander A, Tarkka M, Klopp N, Illig T, Kähönen M, Karhunen PJ, *et al*: miR-21, miR-210, miR-34a, and miR-146a/b are up-regulated in human atherosclerotic plaques in the Tampere Vascular Study. Atherosclerosis 219: 211-217, 2011.
22. Livak KJ and Schmittgen TD: Analysis of relative gene expression data using real-time quantitative PCR and the $2^{-\Delta\Delta CT}$ method. Methods 25: 402-408, 2001.
23. Nicholls DG: Fluorescence measurement of mitochondrial membrane potential changes in cultured cells. Res Gate 810: 119-133, 2012.
24. Zhang X, Xia S, Xu Q and Huang J: The cytoprotective effects of Δ-17 fatty acid desaturase on injured HUVECs and its underlying mechanism. Saudi Pharm J 25: 587-594, 2017.
25. Zhang X, Liu X, Li Y, Lai J, Zhang N, Ming J, Ma X, Ji Q and Xing Y: Downregulation of microRNA-155 ameliorates high glucose-induced endothelial injury by inhibiting NF-κB activation and promoting HO-1 and NO production. Biomed Pharmacother 88: 1227-1234, 2017.
26. Lu J, Mitra S, Wang X, Khaidakov M and Mehta JL: Oxidative stress and lectin-like Ox-LDL-receptor LOX-1 in atherogenesis and tumorigenesis. Antioxid Redox Signal 15: 2301-2333, 2011.
27. Yang F, Li QJ, Gong ZB, Zhou L, You N, Wang S, Li XL, Li JJ, An JZ, Wang DS, *et al*: MicroRNA-34a targets Bcl-2 and sensitizes human hepatocellular carcinoma cells to sorafenib treatment. Technol Cancer Res Treat 13: 77-86, 2014.
28. Li L, Yuan L, Luo J, Gao J, Guo J and Xie X: MiR-34a inhibits proliferation and migration of breast cancer through down-regulation of Bcl-2 and SIRT1. Clin Exp Med 13: 109-117, 2013.
29. Ji R, Cheng Y, Yue J, Yang J, Liu X, Chen H, Dean DB and Zhang C: MicroRNA expression signature and antisense-mediated depletion reveal an essential role of microrna in vascular neointimal lesion formation. Circ Res 100: 1579-1588, 2007.
30. Xu K, Liu P and Zhao Y: Upregulation of microRNA-876 induces endothelial cell apoptosis by suppressing Bcl-Xl in development of atherosclerosis. Cell Physiol Biochem 42: 1540-1549, 2017.
31. Ehara S, Ueda M, Naruko T, Haze K, Itoh A, Otsuka M, Komatsu R, Matsuo T, Itabe H, Takano T, *et al*: Elevated levels of oxidized low density lipoprotein show a positive relationship with the severity of acute coronary syndromes. Circulation 103: 1955-1960, 2001.
32. Jialal I and Devaraj S: The role of oxidized low density lipoprotein in atherogenesis. J Nutr 126 (4 Suppl): 1053S-1057S, 1996.
33. Zheng H, Cui D, Quan X, Yang W, Li Y, Zhang L and Liu E: Lp-PLA2 silencing protects against ox-LDL-induced oxidative stress and cell apoptosis via Akt/mTOR signaling pathway in human THP1 macrophages. Biochem Biophys Res Commun 477: 1017-1023, 2016.
34. Li D and Mehta JL: Antisense to LOX-1 inhibits oxidized LDL-mediated upregulation of monocyte chemoattractant protein-1 and monocyte adhesion to human coronary artery endothelial cells. Circulation 101: 2889-2895, 2000.
35. Li D and Mehta JL: Upregulation of endothelial receptor for oxidized LDL (LOX-1) by oxidized LDL and implications in apoptosis of human coronary artery endothelial cells: Evidence from use of antisense LOX-1 mRNA and chemical inhibitors. Arterioscler Thromb Vasc Biol 20: 1116-1122, 2000.
36. Chen J, Mehta JL, Haider N, Zhang X, Narula J and Li D: Role of caspases in Ox-LDL-induced apoptotic cascade in human coronary artery endothelial cells. Circ Res 94: 370-376, 2004.
37. Chen Z, Wang M, He Q, Li Z, Zhao Y, Wang W, Ma J, Li Y and Chang G: MicroRNA-98 rescues proliferation and alleviates ox-LDL-induced apoptosis in HUVECs by targeting LOX-1. Exp Ther Med 13: 1702-1710, 2017.
38. Zhang Y, Qin W, Zhang L, Wu X, Du N, Hu Y, Li X, Shen N, Xiao D, Zhang H, *et al*: MicroRNA-26a prevents endothelial cell apoptosis by directly targeting TRPC6 in the setting of atherosclerosis. Sci Rep 5: 9401, 2015.
39. Stocker R and Keaney JF Jr: Role of oxidative modifications in atherosclerosis. Physiol Rev 84: 1381-1478, 2004.
40. Madamanchi NR and Runge MS: Mitochondrial dysfunction in atherosclerosis. Circ Res 100: 460-473, 2007.
41. Kregel KC and Zhang HJ: An integrated view of oxidative stress in aging: Basic mechanisms, functional effects, and pathological considerations. Am J Physiol Regul Integr Comp Physiol 292: R18-R36, 2006.
42. Wen H, Gwathmey JK and Xie LH: Oxidative stress-mediated effects of angiotensin II in the cardiovascular system. World J Hypertens 2: 34-44, 2012.
43. Zhang H, Zhao Z, Pang X, Yang J, Yu H, Zhang Y, Zhou H and Zhao J: MiR-34a/sirtuin-1/foxo3a is involved in genistein protecting against ox-LDL-induced oxidative damage in HUVECs. Toxicol Lett 277: 115-122, 2017.
44. Sun HN, Kim SU, Lee MS, Kim SK, Kim JM, Yim M, Yu DY and Lee DS: Nicotinamide adenine dinucleotide phosphate (NADPH) oxidase-dependent activation of phosphoinositide 3-kinase and p38 mitogen-activated protein kinase signal pathways is required for lipopolysaccharide-induced microglial phagocytosis. Biol Pharm Bull 31: 1711-1715, 2008.
45. Li SZ, Hu YY, Zhao J, Zhao YB, Sun JD, Yang YF, Ji CC, Liu ZB, Cao WD, Qu Y, *et al*: MicroRNA-34a induces apoptosis in the human glioma cell line, A172, through enhanced ROS production and NOX2 expression. Biochem Biophys Res Commun 444: 6-12, 2014.
46. Qin B, Xiao B, Liang D, Xia J, Li Y and Yang H: MicroRNAs expression in ox-LDL treated HUVECs: MiR-365 modulates apoptosis and Bcl-2 expression. Biochem Biophys Res Commun 410: 127-133, 2011.
47. Shin S, Chul K, Uk K and Ha E: Biochimie MicroRNA-513a-5p mediates TNF-α and LPS induced apoptosis via downregulation of X-linked inhibitor of apoptotic protein in endothelial cells. Biochimie 94: 1431-1436, 2012.
48. Reuter S, Eifes S, Dicato M, Aggarwal BB and Diederich M: Modulation of anti-apoptotic and survival pathways by curcumin as a strategy to induce apoptosis in cancer cells. Biochem Pharmacol 76: 1340-1351, 2008.
49. Zhao J, Ou SL, Wang WY, Yan C and Chi LX: MicroRNA-1907 enhances atherosclerosis-associated endothelial cell apoptosis by suppressing Bcl-2. Am J Transl Res 9: 3433-3442, 2017.
50. Ji Q, Hao X, Meng Y, Zhang M, Desano J, Fan D and Xu L: Restoration of tumor suppressor miR-34 inhibits human p53-mutant gastric cancer tumorspheres. BMC Cancer 8: 266, 2008.
51. Bommer GT, Gerin I, Feng Y, Kaczorowski AJ, Kuick R, Love RE, Zhai Y, Giordano TJ, Qin ZS, Moore BB, *et al*: p53-mediated activation of miRNA34 candidate tumor-suppressor genes. Curr Biol 17: 1298-1307, 2007.
52. Igney FH and Krammer PH: Death and anti-death: Tumour resistance to apoptosis. Nat Rev Cancer 2: 277-288, 2002.
53. Kapoor R, Rizvi F and Kakkar P: Naringenin prevents high glucose-induced mitochondria-mediated apoptosis involving AIF, Endo-G and caspases. Apoptosis 18: 9-27, 2013.
54. Kim WH, Lee JW, Suh YH, Hong SH, Choi JS, Lim JH, Song JH, Gao B and Jung MH: Exposure to chronic high glucose induces β-cell apoptosis through decreased interaction of glucokinase with mitochondria. Diabetes 54: 2602-2611, 2005.